Adsorption of Pb and Cd in rice husk and their immobilization in porous glass-ceramic structures

Adsorption of Pb and Cd in rice husk and their immobilization in porous glass-ceramic structures

Elham Sharifikolouei*†, Francesco Baino, Camilla Galletti, Debora Fino and Monica Ferraris

Abstract

Rice husk, an agricultural waste, is abundantly available in many countries such as China, India, Brazil, US, and South East Asia. Despite the massive production of rice husk, it is mainly disposed to landfill. In this work, utilization of rice husk for a potential wastewater treatment is evaluated, along with subsequent encapsulation of the adsorbed heavy metals (Pb and Cd) inside a porous glass-ceramic.

Vitrified bottom ash (another source of waste) was mixed with foaming agents in different weight ratios (40:60, 50:50, and 60:40) to prepare a glass matrix for encapsulation of Pb-/Cd-loaded rice husk. It was shown that using 40 wt% vitrified bottom ash with 60 wt% foaming agents leads to a foam glass with the best pore size distribution. Therefore, this batch was further mixed with 70volume% (5 wt%) heavy metal-loaded rice husk and was heat-treated at 750∘C for 3 hours. The final glass-ceramic porous structure was characterized using SEM, XRD, compression test, and it was shown that it is safe to be used as it passes the EN12457-2 leaching test.

Key words: rice hulls, glass-ceramics, porous materials, circular economy

1 Introduction

One of the most serious environmental challenges in the global socioeconomic context is the existence of toxic heavy metals in industrial waste waters. Several methods have been investigated for heavy metal removal from aqueous solutions such as membrane filtration, chemical precipitation, reverse osmosis, ion exchange and adsorption [1-4]. Among these processes, the adsorption process is a simple and effective technique for heavy metal removal from waste water. The most important adsorbents include zeolites [5-7], activated carbon [8-10], expanded perlite [11], and rice husks [12-15]. Even though activated carbon became the most attractive candidate as an adsorbent, but its cost and the loss of adsorption efficiency after regeneration of the exhausted activated carbon [16,

*Corresponding author.
†E-mail: elham.sharifikolouei@polito.it

17] moved the in- investigation toward low-cost green adsorbents [18, 19]. This term is applied to low-cost materials originated from agricultural sources and by-products, or even their waste and residues. Among agricultural residues, rice husk with its unique characteristics is a highly attractive choice. Some of its characteristics are high silica contents (87-97 wt.% SiO2), high porosity, lightweight and very high external surface area[20].

Several works have been done for application of rice husk as an adsorbent. Ajmal et al [15] showed that it is possible to adsorb Ni, Zn, Cd, and Cr by phosphate treating rice husk, and the adsorption was significant in case of Cd and Ni. Amin et al. [21] also showed that it is possible to completely remove As(III) and As(V) from aqueous solutions using rice husk.

It is worth pointing out that the environmental concern does not end after adsorbing heavy metals. In fact, the adsorbed heavy metals need to be encapsulated within a safe structure to prevent further introduction of these elements into the environment. The most common approaches are encapsulation of heavy metals within a glass, glass-ceramic, or cementitious structures [22-25]. The aim of this work is focused on encapsulation of heavy metals adsorbed by rice husk within a porous glass-ceramic structure using vitrified bottom ash from municipal solid waste incinerators (MSWI), which in fact is another products based on waste materials. The reason relied on the economic aspects of treating the rice husk. As already mentioned before, rice husk contains high amount of silica, and its direct vitrification is not economically viable. Similar approaches have been successfully carried out to immobilize hazardous waste from radioactive waste, industrial or hospital waste inside a glass-ceramic structure, using recycled glass to lower down the heat- treatment (sintering) temperature [26, 27].

Encapsulation of heavy metals inside a glass-ceramic structure not only is an excellent option to safely immobilize heavy metals, but it contributes further to the circular economy generating high-added-value products and avoiding waste landfill disposal. This approach is specially emphasized by EU under "A zero waste program for Europe" [28]. It promotes resource efficiency agenda established under the Europe 2020 strategy for establishing a smart and sustainable growth[29]. This approach can lead to significant economic benefits[30]. Therefore, this work is dedicated to using two sources of waste (rice husk and bottom ash) for water treatment and production of porous glass-ceramics.

2 Materials and Methods

2.1 Adsorption of Pb and Cd

The rice husk was provided from a local rice mill in Italy. The pre-treatment was carried out by boiling the rice husk in distilled water at 150◦ C for 5 hours. The resulting product was subsequently washed in distilled water and was dried at 150◦ C for 12 hours. Synthetic waste-water solutions were prepared by dissolving analytical grade Cd(NO3)2.4H2O and PbNO3 in distilled water to obtain a concentration of 5 mg/mL for both Cd and Pb. Further details of experimental procedure for adsorption of Pb and Cd in rice husk could be found at [31]. The elemental analysis of rice husk before and after

adsorption of Pb and Cd was performed by XRF (RIGAKU ZSX100E equipped with a Rh X-ray tube and TAP, PET, LiF1, Ge, RX61 and RX45 analysis crystals). Samples were prepared by pressing ground rice husk into thin discs with a diameter of 20 mm and a thickness of 2 mm. The samples were analyzed in at least 20 different points.

2.2 Preliminary Foam Glass Batches

Three batches were prepared by mixing previously vitrified bottom ash and foaming agents in three different weight ratios(vitrified bottom ash(V): foaming agent(F) = 40:60, 50:50, and 60:40). In this work, these batches are presented by the name 40V60F, 50V50F, and 60V40F, respectively. The detailed composition of the vitrified bottom ash could be found in the work by Bassani et al [32]. Borax ((Na2B4O7).10H2O) and calcium Carbonate were used as softener and foaming agent respectively with the weight ratio of borax:calcium carbonate = 3:1. This ratio was selected based on our previous work on generation of porous Cinderlite [38] The thermal behavior of the batches was studied by hot stage microscopy (Expert System Solution, Modena, Italy). A small compact powder of each batch (diameter $\approx$ 1mm , height $\approx$ 3mm) was placed on a high-purity alumina plate. The powders were then heated up to their melting point, with the heating rate of 10$\circ$C/min. The change of sample dimensions upon heating (shrinkage) was then measured in terms of the silhouette area by using the appropriate image analysis software provided by the manufacturer. Specifically, HSM plots reported the A/A0 ratio vs. temperature, where A was the area of the sample silhouette at a given temperature and A0 was the initial area at 25$\circ$C. After HSM, it was decided to obtain the glass foams 40V60F, 50V50F, and 60V40F by heating up the batches up to 750$\circ$C with the heating rate of 10$\circ$C/min for the dwelling time of 15 min. Optical images of the obtained foam glasses were then captured by optical microscope and were analyzed using particle analysis plugin of Fiji ImageJ [34].

2.3 Encapsulation of Heavy Metals in the Porous Glass-Derived End-of- Waste

After analyzing the result of the three batches and finding the right heat- treatment conditions, the 40V60F batch was selected and 70 volume% (5 wt%) of rice husk was added to it. They were heat treated at 750$\circ$C with the heating rate of 10$\circ$C/min for the dwelling time of 3 hours to obtain the final porous product embedding heavy metals. XRD analysis of the glass- ceramic was carried out using XPert Pro PW3040/60 diffractometer (PANalytical, Eindhoven, The Netherlands) operating at 40 kV/30 mA with Bragg- Brentano geometry, CuKα incident radiation (wavelength λ = 0.15405nm), step size 0.02$\circ$ and fixed counting time of 1s per step. Field Emission Scanning Electron Microscopy (FESEM) was carried out using Zeiss Merlin microscope (equipped with a GEMINI II column and an EDS detector). The compressive strength of the samples was evaluated by performing crushing tests on polished cuboids (MTS System Corp. apparatus, 5-kN cell load, crosshead speed 0.5 mm/min) as the F-to-A ratio, where F (N) was the peak load registered during the test and A (mm2) was the initial cross-sectional area. The elastic modulus was

determined too, from the linear region of the stress-strain response. Prior to the mechanical tests, the six surfaces of the cuboids were polished by using #400 to #1000 SiC grit papers to obtain flat surfaces. Results from the mechanical tests were expressed as mean $\pm$ standard deviation on four measurements. The crushed components after compression test were used to conduct the leaching test according to BS EN 12457-2 compliance test (2002)[35]. Crushed components (95% particle size < 4mm) in distilled water with the ratio of Liquid:Solid = 10:1, were placed inside a shaker (100 rpm, T = 25$\circ$C) for 24 hours. After 24 hours, they were filtered using a 0.2μm membrane filter. The suspensions' concentration of Pb and Cd in the filtered solution was measured using inductively-coupled plasma mass spectrometry (ICP-MS, iCAP Q, ThermoFischer).

3 Results and Discussion

3.1 Rice Husk Characterization

Table 1 shows the XRF analysis of the rice husk before and after adsorption of Pb and Cd. In fact, it confirms the adsorption of Pb and Cd as they constitute 3.31 wt % and 0.25 wt % of rice husk, respectively, after dipping the adsorbent into the simulated waste-water solutions.

TABLE 1
XRF elemental analysis of rice husk before and after adsorption of Cd and Pb. ND stands for Not Detected.

Composition (Wt%)	Rice Husk	Rice Husk + Cd	Rice Husk + Pb
Si	87.70	95.70	92.10
Mg	1.20	0.38	0.48
P	3.36	0.16	0.43
S	0.20	0.16	0.14
K	3.75	0.59	0.56
Ca	2.59	2.00	2.16
Mn	0.81	0.49	0.21
Fe	0.24	0.27	0.27
Cu	0.08	ND	ND
Zn	0.07	ND	0.06
Cd	-	0.25	-
Pb	-	-	3.31
Balance	-	-	0.28
Total	100	100	100

3.2 Foamed Glass Preparation and Analysis

It was shown in the XRF analysis (see Table 1) that rice husk contains a significant amount of silica. This means that the direct vitrification of rice husk to encapsulate the heavy metals requires high temperature. For this reason, it was decided to encapsulate them within an already vitrified system. Therefore, vitrified bottom ash, which in fact is another source of waste and can further contribute to the circular economy itself, was used together with

foaming agents to prepare such system. The softener and foaming agent (borax and calcium carbonate) serve two objectives, i.e. (i) lowering down the required heat-treatment temperature and (ii) providing a base for a lightweight porous glass-ceramic production. The HSM analysis of the mixture of softener and foaming agent is provided in the supplementary materials. Keeping these goals in mind, three batches were prepared using different ratios of vitrified bottom ash and foaming agents. The suitable heat-treatment temperature was decided based on the behavior of the batches under HSM. Figure 1 shows the thermal behavior of 40V60F, 50V50F, and 60V40F glass batches upon heating.

The incorporation of borax and calcium carbonate in the mixes allowed lowering down the melting temperature of the material from above 1250∘C (vitrified bottom ash [31]) to less than 900∘C in all the three batches investigated. Densification phenomena of the compact of powders followed a similar trend, too. Hence, there is an obvious advantage from an economical viewpoint (lower processing temperatures involve more limited costs) and, furthermore, heavy metal-based toxic gaseous products are not developed at this relatively low temperature range. Figure 1 also shows that all the three HSM plots exhibit a well-visible peak at about 710∘C (40V60F) or 740∘C (50V50F and 60V40F). These peaks correspond to expansion phenomena due to the thermal decomposition of borax, which was previously shown to occur just above 700∘C [36]. Samples 40V60F and 50V50F contain higher amount of borax and calcium carbonate; therefore, by rising the temperature they progressively soften faster than the 60V40F. They melt before calcium carbonate has a chance to thermally decompose (Temperature $800 - 850$∘C [37]), and this decomposition plays a role in the foaming process. A quite weak peak associated to CaCO3- induced foaming can be observed in the sample 60V40F at about 825∘C, when the sample starts to melt. From these preliminary HSM observations, the temperature of 750∘C was selected as a compromise to achieve enough densification and adequate foaming effect.

Heating 40V60F, 50V50F, and 60V40F batches up to 750∘C for 15 minutes, produced foamed materials. The binary optical image of the obtained glass-derived materials, and their porosity distribution analysis is presented in Figure 2. The overall porosity for 40V60F, 50V50F, and 60V40F is estimated to be 38%, 34% and 62% respectively. The 60V40F foamed glass contains the largest pores where they are the major contributors to the final porosity of the sample. This brings heterogeneity to the glass, and poor mechanical properties; therefore, it is discarded for further investigation. 40V60F has three categories of pore dimensions (small, medium, large). The smallest pores ($D < 5\mu$m) are distributed more homogeneously while the largest pores ($D > 20\mu$m) are distributed more heterogeneous. 50V50F shows similar pore distribution to that of 40V60F, but it is slightly less porous. Besides, higher number of smaller pores ($D < 5\mu$m) is available in 40V60F. For this reason, 40V60F was selected among three for further incorporation of rice-husk within.

70 volume% (5 wt%) loaded rice husk (rice husk containing heavy metals) was added to 40V60F and was heat treated for 3 hours at 750∘C. Figure 3 shows the optical picture and the SEM images obtained from the final structure after the heat treatment. From these images, it can be seen that firstly, it is a foamed ceramic and the SEM images show 3 categories of pore sizes (diameter) are present within the structure: $D \approx 25\mu$m, $D \approx 350\mu$m,

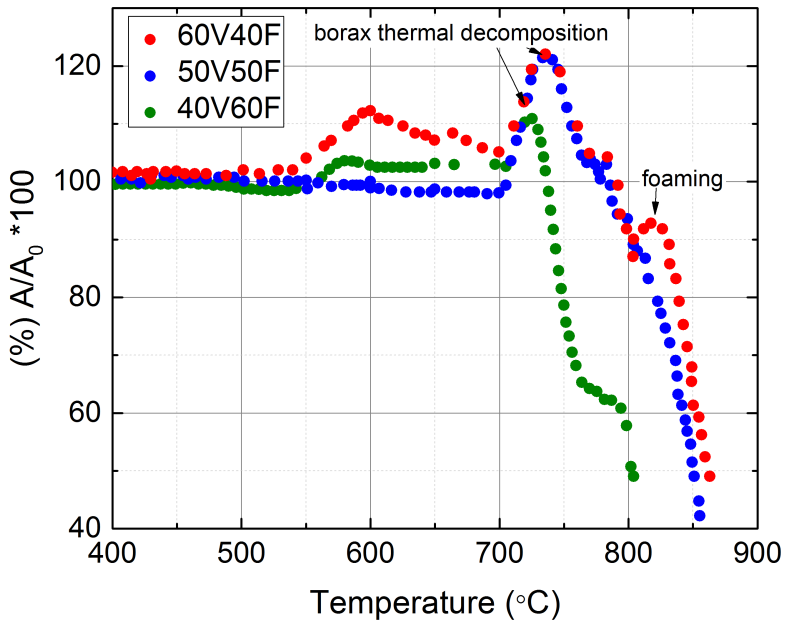

FIGURE 1: HSM plots of 40V60F, 50V50F, and 60V40F batches. All three HSM plots exhibit a well-visible peak at about 710°C(40V60F) or 740°C(50V50F and 60V40F). These peaks correspond to expansion phenomena due to the thermal decomposition of borax. A quite weak peak associated to $CaCO_3$-inducedfoaming can be observed in the sample 60V40F at about 825°C,when the sample starts to melt.

and D $\approx$ 1mm. The smallest pores as well as medium size pores are well distributed within the whole structure. However, the largest pores, as big as several millimeters are accumulated toward the edge of the structure. It is as well noticeable that the large pores are interconnected through small pore windows rather than being isolated; thus, an open-cell glass-derived porous structure was produced.

The XRD analysis of this sample is shown in Figure 4. The main crystalline phases identified to be Calcite, Gehlenite, Cristobalite, Tuscanite, and Jedeite. It is noticeable that these peaks are not sharp and their wide angle could be due to two reasons: 1) the presence of the glassy phase and the nanocrystallinity of the available phases. According to Scherrer formula 1 (where D is the grain size, λ is the Cu$-$Kα wavelength, d is the full width half maximum, and θ is the diffraction position) [38] it is possible to estimate the grain size of the main phases. Putting values in the formula, this size for Jadeite and Tuscanite is estimated to be around 19.5 nm. Besides, the diffusive background between 2θ = 20 $-$ 40$\circ$ indicates the presence of remaining glassy phase. The final structure therefore, is a glass-ceramic.

$$D = \frac{0.9\lambda}{dCos(\theta)} \qquad (1)$$

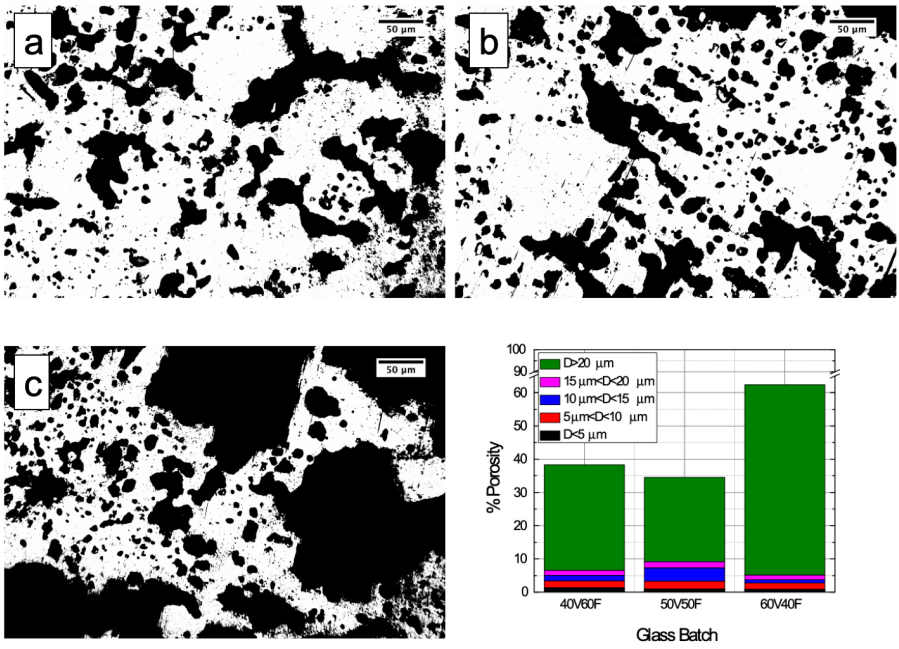

FIGURE 2: Optical images and porosity analysis of 40V60F, 50V50F, and60V40F batches. a) 40V60F has three categories of pores diameters. The smallest pores (D< 5µm) are distributed more homogeneously while the largest pores (D> 20µm) are distributed more heterogeneously b) 50V50F shows similar pore distribution to that of 40V60F, being slightly less porous c) 60V40F shows very heterogeneous pore distribution. This sample has the largest pores (D > 100µm) among all. d)Porosity analysis of 40V60F, 50V50F, and 60V40F. The overall porosity of these batches is estimated to be 38%, 34% and 62%respectively.

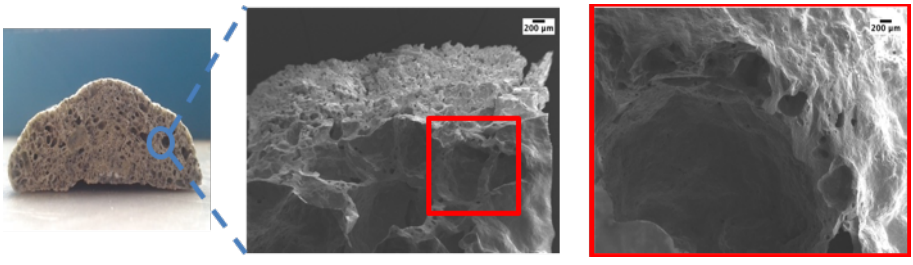

FIGURE 3: Optical picture and SEM images of glass-ceramic obtained after heat-treatment of 70 volume % (5 wt%) of loaded rice husk added to the 40V60F batch at 750°C.

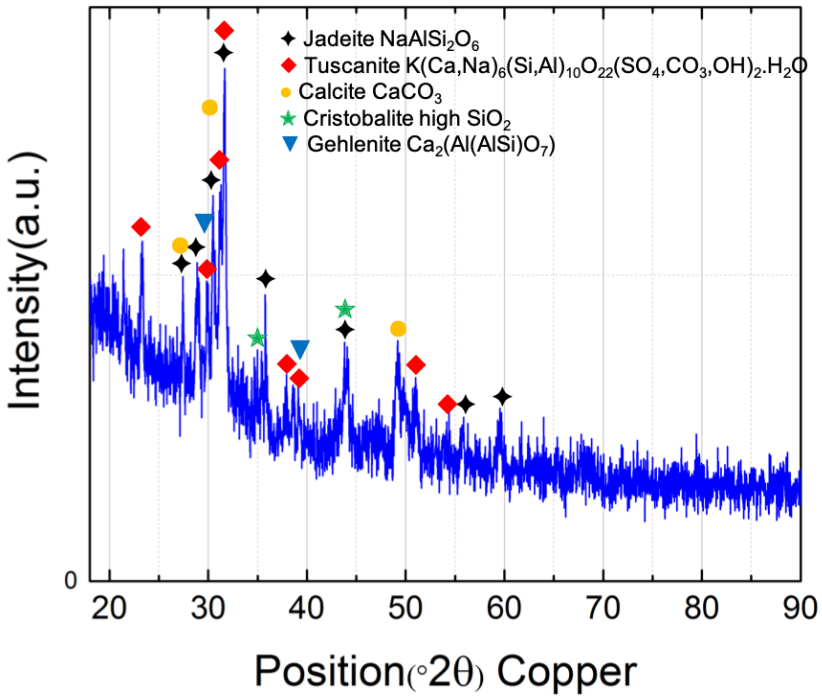

FIGURE 4: XRD analysis of the final structure. The wide peaks and the presence of the diffusive structure between 2θ = 20-40° degree is an indication of remaining glassy phase. The final structure therefore, is a glass-ceramic.

After successful incorporation of rice husk into the glass batch, its applicability in terms of safety and mechanical properties of the resulting porous product was evaluated. The mechanical properties were investigated by compression test. Figure 5 shows the typical stress-strain curve of porous glass- ceramics. Similar curves were obtained in other studies for different types of glass-ceramic foams [38, 39]. The apparent stress drop after the first peak around 10 MPa (marked as point 1) is related to the failure of the thinner struts which crack first under the applied load. However, the material is still able to withstand the load, and this leads to the typical jagged profile of compressive stress-strain curves of cellular ceramics [40]. Then, the stress rises again and a second peak around 7 MPa can be observed (marked as point 2) in Figure 5. After a third broad peak, there is the definite stress drop (marked as point 3) corresponding to the loss of integrity of the sample, which is reduced in powder. The elastic modulus and compressive strength were measured to be 0.950$\pm$0.24 GPa, and 7.5$\pm$1.9 MPa respectively. These mechanical properties suggest safe handling of the materials with no particular problems associated to structural integrity of the glass-ceramic foams. Other authors reported lower values of compressive strength (below 4 MPa) for glass foams from waste glass of dismantled cathode ray tubes [41].

The final test, and the most important of all, regarding the applicability of the glass-ceramic, was leaching test. The leaching test was performed on the crashed pieces after compression test according to the European standard EN12457-2. The concentrations of Pb and Cd, released from the material in aqueous solution, measured by ICP-MS, were 1.71 $\pm$ 0.97 ppb and 1.03 $\pm$ 0.73 ppb respectively. These values are well below the acceptability thresholds recommended by the standard and, thus, this porous glass-ceramic can be considered as an almost inert material [42]. Therefore, the data reported demonstrate that the heavy metals are successfully encapsulated within the glass-ceramic structure and the sample is safe to be used.

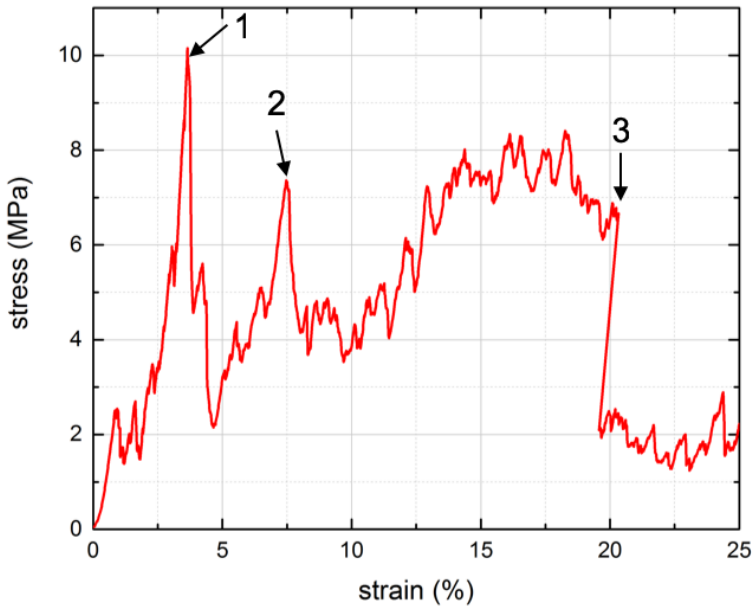

FIGURE 5: Compression on glass-ceramic obtained from mixing 5 Wt% loaded rice husk with 40V60F batch. The apparent stress drops at point 1 but, the material is still able to withstand the load. Then, the stress rises again and a second peak can be observed at point 2. After a third broad peak, there is the definite stress drop ,marked as point 3, corresponding to the loss of integrity of the sample, which is reduced in powder. The elastic modulus and compressive strength were measured to be 0.950 $\pm$ 0.24 GPa, and 7.5 $\pm$1.9 MPa respectively.

4 Conclusions

The current research is conducted as a proof of concept to show the following points in the field of circular economy:

- Instead of landfilling rice-husk as an agricultural waste, it is possible to successfully use it as an adsorbent. This could be an economical option to replace activated carbon for waste water treatment to remove heavy metals.

- To encapsulate the heavy metal loaded-rice husk we have developed a foam glass based on another waste product, incinerator bottom ash. Vitrified bottom ashes were mixed with softener and foaming agent (calcium carbonate and borax) and were heat treated for 15 minutes at 750∘C to make the foam glass, and the best pore size distribution was obtained by mixing 40wt% of vitrified bottom ash and 60wt% of softener-foaming agent mixture.

- The encapsulation of heavy metal-loaded rice husk inside the foam glass was carried out by incorporation of 70 volume% of rice husk into the foam glass, and after 3 hours of heat treatment at 750∘C, a porous structure was obtained which was proved by XRD to be a glass-ceramic.

- The final glass-ceramic passed the standard leaching test EN12457-2, which is an indication of fixed heavy metals within the structure.

- The final structure shows the compressive strength of 7.5 MPa.

In conclusion, this material could be utilized in different applications such as lightweight building materials, materials for thermal and acoustic insulations, and therefore it can be improved for specific applications.

5 References

[1] M. Kobya, U. Gebologlu, F. Ulu, S. Oncel, E. Demirbas, Removal of arsenic from drinking water by the electrocoagulation using fe and al electrodes, Electrochimica Acta 56 (2011) 5060 – 5070.

[2] L. Mafu, T. Msagati, B. Mamba, The enrichment and removal of arsenic (iii) from water samples using hfslm, Physics and Chem- istry of the Earth, Parts A/B/C 50-52 (2012) 121 – 126. 12th WaterNet/WARFSA/GWP-SA Symposium: Harnessing the rivers of knowledge for socio-economic development, climate adaptation envi- ronmental sustainability.

[3] P. Smedley, D. Kinniburgh, A review of the source, behaviour and distribution of arsenic in natural waters, Applied Geochemistry 17 (2002) 517 – 568.

[4] N. Abdullah, N. Yusof, W. Lau, J. Jaafar, A. Ismail, Recent trends of heavy metal removal from water/wastewater by membrane technologies, Journal of Industrial and Engineering Chemistry (2019).

[5] M. Hong, L. Yu, Y. Wang, J. Zhang, Z. Chen, L. Dong, Q. Zan, R. Li, Heavy metal adsorption with zeolites: The role of hierarchical pore ar- chitecture, Chemical Engineering Journal 359 (2019) 363 – 372.

[6] E. Zanin, J. Scapinello, M. de Oliveira, C. L. Rambo, F. Franscescon, L. Freitas, J. M. M. de Mello, M. A. Fiori, J. Oliveira, J. D. Magro, Adsorption of heavy metals from

wastewater graphic industry using clinoptilolite zeolite as adsorbent, Process Safety and Environmental Protection 105 (2017) 194 – 200.

[7] S. S. Obaid, D. Gaikwad, M. Sayyed, K. AL-Rashdi, P. Pawar, Heavy metal ions removal from waste water bythe natural zeolites, Materials Today: Proceedings 5 (2018) 17930 – 17934. Materials Processing and characterization, 16th 18th March 2018.

[8] F. Cao, C. Lian, J. Yu, H. Yang, S. Lin, Study on the adsorption performance and competitive mechanism for heavy metal contaminants removal using novel multi-pore activated carbons derived from recyclable long-root eichhornia crassipes, Bioresource Technology 276 (2019) 211 – 218.

[9] A. Wahby, Z. Abdelouahab-Reddam, R. ElMail, M. Stitou, J. Silvestre- Albero, A. Sepúlveda-Escribano, F. Rodŕıguez-Reinoso, Mercury re- moval from aqueous solution by adsorption onactivated carbons pre- pared from olive stones, Adsorption 17 (2011) 603–609.

[10] M. Karnib, A. Kabbani, H. Holail, Z. Olama, Heavy metals removal using activated carbon, silica and silica activated carbon composite, Energy Procedia 50 (2014) 113 – 120. Technologies and Materials for Renewable Energy, Environment and Sustainability (TMREES14 EU- MISD).

[11] H. Ghassabzadeh, A. Mohadespour, M. Torab-Mostaedi, P. Zaheri, M. G. Maragheh, H. Taheri, Adsorption of ag, cu and hg from aqueous solutions using expanded perlite, Journal of Hazardous Materials 177 (2010) 950 – 955.

[12] A. C. Chiu, R. Akesseh, I. M. Moumouni, Y. Xiao, Laboratory assess- ment of rice husk ash (rha) in the solidification/stabilization of heavy metal contaminated slurry, Journal of Hazardous Materials 371 (2019) 62 – 71.

[13] M. Xu, P. Yin, X. Liu, Q. Tang, R. Qu, Q. Xu, Utilization of rice husks modified by organomultiphosphonic acids as low-cost biosorbents for enhanced adsorption of heavy metal ions, Bioresource Technology 149 (2013) 420 – 424.

[14] N. H. Shalaby, E. M. Ewais, R. M. Elsaadany, A. Ahmed, Rice husk templated water treatment sludge as low cost dye and metal adsorbent, Egyptian Journal of Petroleum 26 (2017) 661 – 668.

[15] M. Ajmal, R. A. K. Rao, S. Anwar, J. Ahmad, R. Ahmad, Adsorption studies on rice husk: removal and recovery of cd(ii) from wastewater, Bioresource Technology 86 (2003) 147 – 149. 10

[16] V. C. Srivastava, I. D. Mall, I. M. Mishra, Adsorption thermodynamics and isosteric heat of adsorption of toxic metal ions onto bagasse fly ash (bfa) and rice husk ash (rha), Chemical Engineering Journal 132 (2007) 267 – 278.

[17] S. Abo-El-Enein, M. Eissa, A. Diafullah, M. Rizk, F. Mohamed, Re- moval of some heavy metals ions from wastewater by copolymer of iron and aluminum impregnated with active silica derived from rice husk ash, Journal of Hazardous Materials 172 (2009) 574 – 579.

[18] G. Kyzas, M. Kostoglou, Green adsorbents for wastewaters: A critical review, Materials 7 (2014) 333–364.

[19] G. M. Al-Senani, F. F. Al-Fawzan, Adsorption study of heavy metal ions from aqueous solution by nanoparticle of wild herbs, The Egyptian Journal of Aquatic Research 44 (2018) 187–194.

[20] N. Soltani, A. Bahrami, M. I. Pech-Canul, L. A. Gonźalez, Review on the physic-ochemical treatments of rice husk for production of advanced materials, Chemical Engineering Journal 264 (2015) 899–935.

[21] M. N. Amin, S. Kaneco, T. Kitagawa, A. Begum, H. Katsumata, T. Suzuki, K. Ohta, Removal of arsenic in aqueous solutions by adsorp- tion onto waste rice husk, Industrial & Engineering Chemistry Research 45 (2006) 8105–8110.

[22] J. Silva Romano, F. Rodrigues, Cements obtained from rice hull: En- capsulation of heavy metals, Journal of hazardous materials 154 (2008) 1075–80.

[23] L. Mao, H. Guo, W. Zhang, Addition of waste glass for improving the immobilization of heavy metals during the use of electroplating sludge in the production of clay bricks, Construction and Building Materials 163 (2018) 875 – 879.

[24] L. Mao, Y. Wu, W. Zhang, Q. Huang, The reuse of waste glass for enhancement of heavy metals immobilization during the introduction of galvanized sludge in brick manufacturing, Journal of Environmental Management 231 (2019) 780 – 787.

[25] H. Song, L. Wei, Y. Ji, L. Cao, F. Cheng, Heavy metal fixing and heat resistance abilities of coal fly ash-waste glass based geopolymers by hydrothermal hot pressing, Advanced Powder Technology 29 (2018) 1487 – 1492.

[26] P. Stoch, M. Cieciska, A. Stoch, ukasz Kuterasiski, I. Krakowiak, Im- mobilization of hospital waste incineration ashes in glass-ceramic com- posites, Ceramics International 44 (2018) 728 – 734.

[27] K.-W. Kim, R. I. Foster, J. Kim, H.-H. Sung, D. Yang, W.-J. Shon, M.- K. Oh, K.-Y. Lee, Glass-ceramic composite wasteform to immobilize and stabilize a uranium-bearing waste generated from treatment of a spent uranium catalyst, Journal of Nuclear Materials 516 (2019) 238 – 246.

[28] M. Smol, J. Kulczycka, A. Avdiushchenko, Circular economy indicators in relation to eco-innovation in european regions, Clean Technologies and Environmental Policy 19 (2017) 669–678.

[29] M. Quaghebeur, B. Laenen, D. Geysen, P. Nielsen, Y. Pontikes, T. V. Gerven, J. Spooren, Characterization of landfilled materials: screening of the enhanced landfill mining potential, Journal of Cleaner Production 55 (2013) 72 – 83. Special Volume: Urban and Landfill Mining.

[30] M. Smol, J. Kulczycka, A. Henclik, K. Gorazda, Z. Wzorek, The possible use of sewage sludge ash (ssa) in the construction industry as a way towards a circular economy, Journal of Cleaner Production 95 (2015) 45 – 54.

[31] F. D. Galletti Camilla, Russo Nunzio, Journal of Chemical Engineering Research Studies

[32] M. Bassani, E. Santagata, O. Baglieri, M. Ferraris, M. Salvo, A. Ven- trella, Use of vitrified bottom ashes of municipal solid waste incinerators in bituminous mixtures in substitution of natural sands, Advances in Applied Ceramics 108 (2009) 33–43.

[33] F. Baino, M. Ferraris, Production and characterization of ceramic foams derived from vitrified bottom ashes, Materials Letters 236 (2019) 281 – 284.

[34] J. Schindelin, I. Arganda-Carreras, E. Frise, V. Kaynig, M. Longair, T. Pietzsch, S. Preibisch, C. Rueden, S. Saalfeld, B. Schmid, J.-Y. Tin- evez, D. J. White, V. Harten-

stein, K. Eliceiri, P. Tomancak, A. Cardona, Fiji: an open-source platform for biological-image analysis, Na- ture Methods 9 (2012) 676.

[35] British-Standard-Institution, En 12457-2, characterization of waste, leaching-compliance test for leaching of granular waste materials and sludges, part 2: One stage batch test at a liquid to solid ratio of 10 l/kg for materials with particle size below 4mm (2002).

[36] I. Waclawska, Thermal decomposition of borax, Journal of Thermal Analysis 43 (1995) 261–269.

[37] I. Galan, C. Andrade, P. Mora, M. A. Sanjuan, Sequestration of CO2 by Concrete Carbonation, Environmental Science & Technology 44 (2010) 3181–3186.

[38] J. I. Langford, A. J. C. Wilson, Scherrer after sixty years: A survey and some new results in the determination of crystallite size, Journal of Applied Crystallography 11 (1978) 102–113.

[39] W. Huo, X. Zhang, Y. Chen, Y. Lu, J. Liu, S. Yan, J.-M. Wu, J. Yang, Novel mullite ceramic foams with high porosity and strength using only fly ash hollow spheres as raw material, Journal of the European Ceramic Society 38 (2018) 2035 – 2042.

[40] L. Gibson, Modelling the mechanical behavior of cellular materials, Materials Science and Engineering: A 110 (1989) 1 – 36.

[41] E. Bernardo, F. Albertini, Glass foams from dismantled cathode ray tubes, Ceramics International 32 (2006) 603–608.

[42] X. Dou, F. Ren, M. Q. Nguyen, A. Ahamed, K. Yin, W. P. Chan, V. W.-C. Chang, Review of mswi bottom ash utilization from perspec- tives of collective characterization, treatment and existing application, Renewable and Sustainable Energy Reviews 79 (2017) 24 – 38.